

Photochemistry in microemulsions: fluorescence quenching of naphthols by some γ -picolinium salts

M. Panda, P.K. Behera, B.K. Mishra, G.B. Behera*

Center of Studies in Surface Science and Technology, Department of Chemistry, Sambalpur University, Jyoti Vihar 768 019, India

Accepted 15 August 1997

Abstract

The fluorescence quenching behaviour of naphthols by some water-soluble quenchers like (methylene)_n bis-(γ -picolinium bromide) and 1-hexyl γ -picolinium bromide have been studied in aqueous medium, and in both water-rich and oil-rich regions of NaLS (sodium lauryl sulfate)–isobutanol–hexane–water and CTAB (cetyltrimethyl ammonium bromide)–isobutanol–hexane–water microemulsion systems. From the fluorescence quenching behaviour, the localization sites of the fluorescent probes in microemulsions have been identified. The charge on the surfactant head group has been found to have significant effect on the quenching phenomena of the naphthols by the pyridinium salts. Both linearity and deviation from linearity in Stern–Volmer plots have been observed during the quenching process and a sphere of action model has been proposed for positive deviation. © 1998 Elsevier Science S.A.

Keywords: Microemulsions; Naphthols; Alkyoxynaphthalenes; γ -Picolinium salts; Dynamic quenching; 'Quenching sphere of action'; Transient quenching; 1-Naphthol; 2-Naphthol; γ -Picolinic; *n*-Alkyl bromide; Dibromoalkane; NaLS; CTAB

1. Introduction

Microemulsion is an isotropic, transparent and thermodynamically stable dispersion of water, oil and emulsifier. It provides four domains; the core (aqueous or organic phase), mesophase (the surfactant layer which acts as a membrane system), interfacial region and the bulk organic or aqueous phase [1]. The ability of the microemulsions to dissolve and compartmentalize both polar and non-polar reactants has a significant effect on chemical reactivity and quenching processes. Being a ternary or quaternary system, it has the advantage of offering better compartmentalization than the other organized assemblies.

With a view to study the effect of compartmentalization of the species in microemulsions, the fluorescence quenching behaviour of 1- and 2-naphthol with various quenchers like CCl_4 (an oil-soluble quencher which can reside in the oil phase or at the mesophase) [2] and Cu^{++} (a divalent water-soluble quencher with concentrated charge) [3] have been reported earlier. When CCl_4 is used as the quencher, a collisional quenching process is proposed from the linear Stern–Volmer plots. In this case, the naphthols and the quencher reside in the same compartment [2]. With Cu^{++} as the quencher, the Stern–Volmer plots deviate from linearity

which has been explained by a sphere of action model. Further, different radii of spheres of action during the quenching process have been obtained for both the naphthols. However, microemulsions with various composition of its constituents could not be obtained due to their instability in presence of Cu^{++} . Since divalent counter ions with concentrated charge (e.g., Cu^{++}) or diffuse charge (e.g., MV^{++}) show similar rheological behaviour in micellar medium [4], in the present work, a set of water soluble quenchers with divalent diffuse charges separated by spacers have been used to replace Cu^{++} . The new set of quenchers have varied hydrophobicity and it may lead to provide differential localization sites with varied distance from the fluorophore. To vary the localization sites of fluorophores in microemulsion media, alkyl groups with varied length have been linked to naphthols, and the resulted *O*-alkyl naphtholates have been used to study the quenching behaviour in oil-in-water (O/W) and water-in-oil (W/O) microemulsions of both cationic and anionic surfactants.

2. Experimental details

The syntheses of *O*-alkyl derivatives of 1- and 2-naphthol have been reported earlier [5].

* Corresponding author.

Table 1
Characterization data of bis-(γ -picolinium bromide)

Compound	Melting point ^a / boiling point ^b (°C)	Yield (%)	Found (calcd.) (%)			
			C	H	N	Br
BPM	264–265 ^c	95	43.29(43.33)	4.40(4.44)	7.75(7.78)	44.44(44.45)
BPE	300–302 ^c	91	44.90(44.92)	4.80(4.81)	7.44(7.49)	42.73(42.78)
BPB	96–100 ^c	85	47.70(47.76)	5.45(5.47)	6.93(6.97)	39.78(39.80)
BPH	89–91 ^c	88	50.14(50.23)	6.03(6.03)	6.48(6.51)	37.20(37.21)
MPH	111–114 ^d	90	55.80(55.81)	7.72(7.75)	5.40(5.43)	31.00(31.01)

Table 2
Formulation of A and B for the NaLS and CTAB microemulsions

		Surfactant (% w/w)	Isobutanol (% w/w)	Hexane (% w/w)	Water (% w/w)
NaLS	A	11.7	28.1	44.7	15.5
	B	11.9	28.6	8.0	51.5
CTAB	A	11.7	28.1	44.6	15.6
	B	11.7	28.2	5.3	54.8

2.1. Synthesis of 1,1'-methylene bis-(γ -picolinium bromide) (BPM)

A mixture of γ -picoline (0.93 g, 0.01 mol) and 1,1'-dibromomethane (0.87 g, 0.05 mol) was refluxed on a water bath for 6 h. A white solid separated which was washed with diethyl ether. The salt was crystallized thrice from water–alcohol mixture and was kept in the desiccator.

1-Hexyl γ -picolinium bromide (MPH), 1,2-ethylene bis-(γ -picolinium bromide) (BPE), 1,4-butylene bis-(γ -picolinium bromide) (BPB) and 1,6-hexylene bis-(γ -picolinium bromide) (BPH) were synthesized by the same method as BPM. All the salts except MPH were crystallized from water–alcohol mixture. 1-Hexyl γ -picolinium bromide was purified by column chromatography. The analytical data of the synthesized compounds are given in Table 1. The bromide ions in the salts were determined by Volhard's Method [6].

The microemulsions were prepared by stirring the various components in appropriate amount with a mechanical stirrer. The order of mixing of the components of microemulsion has no effect on the stability of the microemulsion. Sodium lauryl sulphate (Sigma) was crystallized twice from alcohol. Isobutanol (Merck) was distilled twice before use. Hexane was distilled twice in a fractionating column. Triply distilled water was used throughout the study. 1-Naphthol and 2-naphthol (Sisco Chem) were purified by subliming twice after crystallization from alcohol. The solutions were deoxygenated by passing dry nitrogen gas before the experiment.

Absorption and fluorescence spectra were recorded by UV-Vis Shimadzu—160 A spectrophotometer and Shimadzu RF-5000 spectrofluorimeter, respectively. Narrow

excitation and emission slit widths (half band width = 1.5 nm) were chosen. The concentration of 1- and 2-naphthol in the solution were maintained at 1×10^{-4} M. The quencher (BPM, BPE, BPB, BPH and MPH) concentration was varied in the range 0–0.02 M.

The pseudo-ternary phase diagram constructed by visual titration of the mixtures of NaLS–isobutanol–hexane–water and CTAB–isobutanol–hexane–water have been described earlier [7]. In the present study the formulations for NaLS and CTAB microemulsions are given in Table 2.

3. Results and discussion

3.1. Absorption and fluorescence spectra

The absorption and emission spectral data of the naphthols (ROH) and their *O*-alkyl derivatives (ROR') in various media are given in Tables 3 and 5. The emission peak of 1-ROH around 336–356 nm is due to the molecular species (1-ROH*), whereas the peak around 456–462 nm is due to the dissociated 1-RO^{-*}. The extent of dissociation is found to increase with increasing amount of water in the medium. In pure organic solvents 1-ROH* does not dissociate, but in the alcohol–water mixture the dissociation increases with increasing water content (Fig. 1) and becomes complete in pure water.

By monitoring the intensity at the maximum wavelength of emission spectra for 1-RO^{-*} the extent of dissociation have been determined. In O/W ME, the dissociation of 1-ROH* is found to be 26% in NaLS and 70% in CTAB surfactant system whereas in W/O ME the extent of dissociation decreases to 12% and 49%, respectively. Microemulsions provide microenvironments with varying polarity and 1-ROH is supposed to partition more to the nonpolar environment ($K_{\text{hexane/water}} = 2.7$). When the extent of dissociation of 1-ROH* in both the microemulsions is compared with that in ethanol–water mixture, the environment of 1-ROH in the W/O ME and O/W ME of the NaLS surfactant system corresponds to 95% and 88% ethanol:water(v/v) respectively. The corresponding values in CTAB microemulsion is similar to 75% and 60% ethanol:water(v/v) in W/O and O/W ME

Table 3

λ_{\max} , λ_{ex} , λ_{em} (nm) and Fluorescence intensity values of naphthols in different environments (log ϵ values are given in parentheses), [ROH] = 1×10^{-4} M

Fluorophore	Environment	λ_{\max} in nm (log ϵ , mol ⁻¹ cm ²)	λ_{ex}	λ_{em}	Intensity	
1-ROH	Hexane	291 (3.72)	291	336	134.33	
	O/W ME (NaLS)	297 (3.65)	297	356	43.96	
	W/O ME (NaLS)	297 (3.70)	297	356	82.99	
	O/W ME (CTAB)	297 (3.74)	297	356	32.96	
	W/O ME (CTAB)	297 (3.83)	297	355	52.41	
	Water ^d	292 (3.74)	292	462	37.05	
	Ethanol	297 (3.70)	297	355	133.82	
	Methanol	297 (3.77)	297	355	166.84	
	2-ROH	Hexane	328 (3.39)	330	346	134.31
		O/W ME (NaLS)	331 (3.30)	330	354	201.50
W/O ME (NaLS)		330 (3.36)	330	354	152.20	
O/W ME (CTAB)		331 (3.34)	330	354	129.72	
W/O ME (CTAB)		331 (3.35)	330	354	139.71	
Ethanol		331 (3.34)	330	354	160.70	
Methanol		331 (3.33)	330	352	144.32	
Water ^d		328 (3.22)	330	352	145.08	
				416	64.14	

^d0.2% methanol in case of 1- and 2-ROH.

Table 4

λ_{\max} (nm) Values of 1- and 2-naphthol and their *O*-alkyl derivatives in hexane and water-rich region of NaLS and CTAB microemulsions (log ϵ values are given in parentheses)

Fluorophores	λ_{\max} in nm (log ϵ , mol ⁻¹ cm ²)		
	Hexane	NaLS ME	CTAB ME
1-ROH	291 (3.72)	297 (3.65)	297 (3.74)
1-ROCH ₃	292 (3.79)	292 (3.74)	293 (3.82)
1-ROC ₄ H ₁₀	294 (3.77)	294 (3.74)	294 (3.83)
1-ROC ₁₂ H ₂₅	294 (3.73)	294 (3.67)	294 (3.77)
1-ROC ₁₆ H ₃₃	294 (3.78)	294 (3.73)	294 (3.83)
1-ROC ₁₈ H ₃₇	293 (3.79)	294 (3.76)	294 (3.74)
2-ROH	328 (3.39)	331 (3.30)	331 (3.34)
2-ROCH ₃	327 (3.38)	327 (3.21)	328 (3.44)
2-ROC ₄ H ₁₀	328 (3.39)	328 (3.29)	328 (3.22)
2-ROC ₁₂ H ₂₅	328 (3.40)	328 (3.30)	328 (3.24)
2-ROC ₁₆ H ₃₃	328 (3.35)	328 (3.28)	328 (3.20)
2-ROC ₁₈ H ₃₇	328 (3.39)	328 (3.28)	328 (3.39)

respectively. The increase in polarity in O/W ME over W/O ME may be attributed to more water penetration into the mesophase of microemulsion droplet. The increase in dissociation in the cationic microemulsion is due to electrostatic effect.

On excitation, the dissociation of 2-ROH is found to be significantly less than 1-ROH [8–10]. In aqueous medium it

dissociates to an extent of 33%, whereas in organic solvents and in microemulsions no dissociation is observed. However, in water–ethanol mixture the dissociation increases with increasing amount of water in the medium (Fig. 1). No dissociation of 2-ROH in microemulsions indicates that the environment of 2-ROH in the microemulsions are ethanolic. Thus 2-ROH remains at a greater distance from the interface than 1-ROH. Georges [11] has also reported a decrease in dissociation of excited 2-ROH in ionic micelles when compared to aqueous medium.

In microemulsions (O/W and W/O ME) and hexane, the values of λ_{\max} and the nature of the spectra remain the same for the alkoxy-naphthalenes. Therefore, all the alkyl derivatives have hexane-like environment in the microemulsions. From Table 5, it is observed that although λ_{em} values of the *O*-alkoxy derivatives are same for all the media, the fluorescence intensity values increase in the order hexane < CTAB O/W ME < NaLS O/W ME. Fluorescence intensity is enhanced in organized medium [5,11] probably because the microenvironment of the solute in the microemulsion is different from that in the pure solvent.

3.2. Fluorescence quenching

The shape of the fluorescence spectra with and without the quencher remains the same with no change in the position of

Table 5

λ_{ex} , λ_{em} (nm) and Fluorescence intensity (I) values of 1- and 2-naphthol and their *O*-alkyl derivatives in hexane and water-rich region of NaLS and CTAB microemulsions

Fluorophores	Hexane			NaLS ME			CTAB ME		
	λ_{ex}	λ_{em}	I_{em}	λ_{ex}	λ_{em}	I_{em}	λ_{ex}	λ_{em}	I_{em}
1-ROH	290	336.0	134.33	297	356.0	43.96	297	356.8	32.96
1-ROCH ₃	290	334.0	126.64	290	456.0	15.55	290	451.2	74.94
1-ROC ₆ H ₁₉	290	334.8	124.20	290	335.0	245.50	290	355.0	233.66
1-ROC ₁₂ H ₂₅	290	334.8	124.22	290	335.6	213.31	290	335.6	181.95
1-ROC ₁₆ H ₃₃	290	335.2	128.20	290	335.6	212.28	290	335.6	208.57
1-ROC ₁₈ H ₃₇	290	335.2	127.20	290	335.6	223.55	290	335.6	211.64
2-ROH	330	346.0	134.31	290	336.0	216.25	290	335.6	199.36
2-ROCH ₃	330	342.4	138.97	330	354.0	201.50	330	354.4	129.72
2-ROCH ₃	330	342.4	138.97	330	344.0	212.67	330	344.0	150.20
2-ROC ₆ H ₁₉	330	343.6	135.87	330	344.8	203.30	330	344.4	134.33
2-ROC ₁₂ H ₂₅	330	343.6	135.31	330	344.8	217.28	330	344.4	140.48
2-ROC ₁₆ H ₃₃	330	343.6	131.80	330	344.8	203.58	330	344.4	129.72
2-ROC ₁₈ H ₃₇	330	343.6	139.94	330	344.8	214.72	330	344.4	145.60

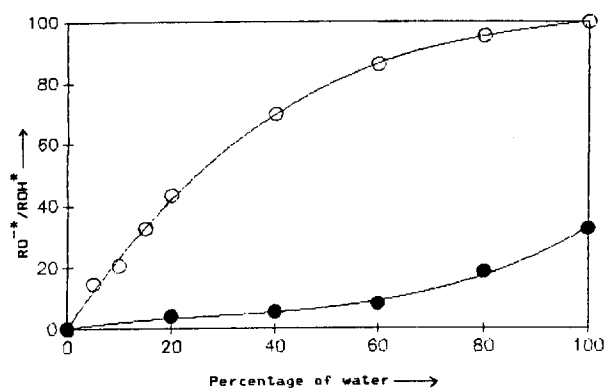


Fig. 1. Percentage of dissociation of 1-naphthol (○) and 2-naphthol (●) in various water-ethanol mixture.

the maxima. Observation of similar absorption spectra of a solution with the quencher, after carrying out the fluorescence, indicates that no detectable photoproduct is formed under the experimental conditions. The absence of any new fluorescence peak at longer wavelength discards the possibility of complexation of the naphthols with the quenchers. The decrease of the fluorescence intensity of all the fluorophores without the appearance of any new band in the presence of the quencher indicates that no emissive exciplex is formed between fluorophores and quenchers in the experimental condition.

3.3. Stern–Volmer (SV) plot

The I_0/I values for all the systems (1-ROH*, 1-RO^{-*}, 2-ROH*, 2-RO^{-*}, 1-ROR'* and 2-ROR'* in water and microemulsions) have been correlated with the quencher concentration, $[Q]$, by using the Stern–Volmer (SV) equation [12] (Eq. (1)).

$$I_0/I - 1 = K_{SV} [Q] \quad (1)$$

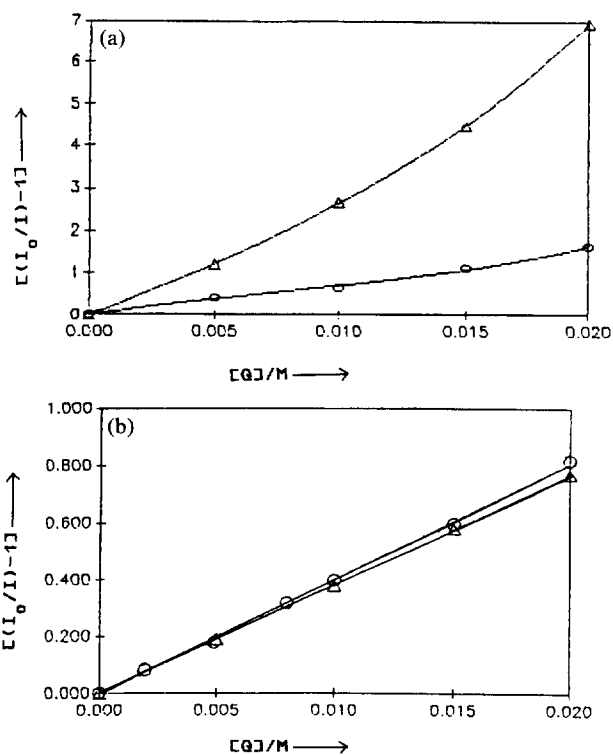


Fig. 2. (a) Stern–Volmer Plots for the fluorescence quenching of 2-ROH* (○) and 2-RO^{-*} (Δ) by BPM salt in aqueous medium. (b) Stern–Volmer Plots for the fluorescence quenching of 2-ROH* by BPM salt in oil-in-water (○) and water-in-oil (Δ) NaLS microemulsion system.

In this equation, I_0 and I are the fluorescence intensities of the fluorophores in the absence and presence of the quencher respectively, K_{SV} is the Stern–Volmer constant.

Some representative Stern–Volmer plots are presented in Fig. 2. It has been observed that except for 2-ROH in both W/O and O/W MEs, all the plots deviate from linearity. The K_{SV} values obtained for 2-ROH in NaLS microemulsions are

Table 6

The Stern–Volmer (K_{SV})^a and transient (K_T) quenching constant values (in mol⁻¹ dm³) for ROH*–salt systems in different environments at 27°C

Fluorophore	BPM	BPE	BPB	BPH	MPH
1-RO ⁻ (H ₂ O)	126.70	99.20	92.99	96.35	52.50
1-ROH (O/WME,NaLS)	22.08	26.62	20.85	18.70	11.96
1-RO ⁻ (O/WME,NaLS)	55.77	49.78	46.32	43.20	25.54
1-ROH (W/OME,NaLS)	57.00	36.80	20.06	24.70	19.21
1-ROH (O/WME,CTAB)	120.50	nq	nq	nq	11.37
1-RO ⁻ (O/WME,CTAB)	151.33	nq	nq	nq	34.37
1-ROH (W/OME,CTAB)	219.00	nq	nq	nq	46.90
1-RO ⁻ (W/OME,CTAB)	309.00	128.00	nq	nq	46.50
2-ROH (H ₂ O)	48.44	46.40	44.68	47.83	32.90
2-RO ⁻ (H ₂ O)	87.80	80.40	81.70	81.82	73.27
2-ROH (O/WME,NaLS)	40.90 ^a	42.44 ^a	35.31 ^a	42.80 ^a	26.07
2-ROH (W/OME,NaLS)	38.60 ^a	45.60 ^a	34.20 ^a	43.20 ^a	23.26
2-ROH (O/WME,CTAB)	nq	nq	nq	nq	16.04
2-ROH (W/OME,CTAB)	nq	nq	nq	nq	20.71

*nq: No appreciable quenching.

3.4. Deviation in Stern–Volmer plots

In the absence of any chemical reaction of the excited fluorophore, the deviation from the linearity may be due to (i) ground state complex formation or (ii) transient quenching. Deviation due to ground state complex formation is ruled out as no change is observed in the absorption spectra in presence of quencher. Hence transient quenching due to the presence of a quenching sphere of action may be proposed for the quenching phenomenon. According to the quenching sphere of action model [13–15],

$$I_0/I = \exp(K_T [Q]) \quad (2)$$

Eq. (2) can be written as,

$$\ln I_0/I = K_T [Q] = vN[Q] \quad (3)$$

where K_T is the transient quenching constant, v is the volume of the transient quenching sphere, N is the Avogadro's number.

The plots of $\ln I_0/I$ vs. $[Q]$ are found to be linear ($r \geq 0.99$) (Fig. 3). The K_T values obtained from the plots and the radii of the quenching sphere of action (taking $K_T = vN$) have been determined and are given in Tables 6, 7 and 8.

3.5. 1-RO^{-*}, 2-ROH* and 2-RO^{-*} in aqueous medium

1-ROH on excitation dissociates completely in aqueous medium and, therefore, the quenching parameters of 1-ROH* could not be determined. The K_T values (or R values) for 1-RO^{-*}, 2-ROH* and 2-RO^{-*} with all the quencher salts are in the order: 1-RO^{-*} > 2-RO^{-*} > 2-ROH*. The quenchers are dipositive like Cu²⁺ ion, but have hydrophobic spacer. The K_T values are found to drop from BPM to BPE and then remain almost constant for all the fluorophores with increasing spacer between the two picolinium moieties. The

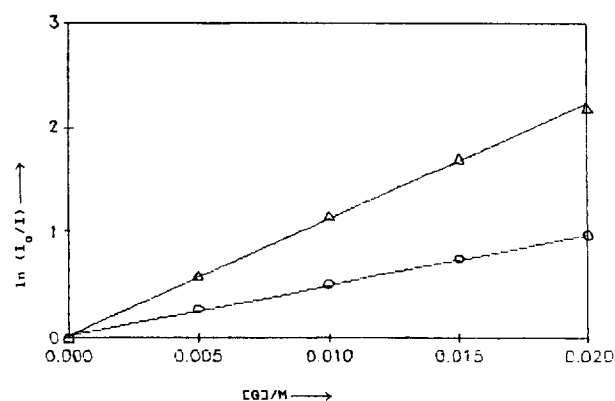
Fig. 3. Plot of $\ln(I_0/I)$ vs. $[Q]$ for the fluorescence quenching of 2-ROH* (O) and 2-RO^{-*} (Δ) in aqueous medium.

Table 7

Radius of the 'Quenching sphere of action' (in nm) for ROH–salt systems in different environments at 27°C

Fluorophore	BPM	BPE	BPB	BPH	MPH
1-RO ⁻ (H ₂ O)	3.69	3.40	3.32	3.37	2.75
1-ROH (O/WME,NaLS)	2.06	2.19	2.02	1.95	1.68
1-RO ⁻ (O/WME,NaLS)	2.81	2.70	2.64	2.58	2.16
1-ROH (W/OME,NaLS)	2.83	2.44	2.00	2.14	1.97
1-ROH (O/WME,CTAB)	3.63	—	—	—	1.65
1-RO ⁻ (O/WME,CTAB)	3.91	—	—	—	2.39
1-ROH (W/OME,CTAB)	4.43	—	—	—	2.65
1-RO ⁻ (W/OME,CTAB)	4.97	3.70	—	—	2.52
2-ROH (H ₂ O)	2.68	2.64	2.61	2.67	2.35
2-RO ⁻ (H ₂ O)	3.26	3.17	3.19	3.19	3.07
2-ROH (O/WME,NaLS)	—	—	—	—	2.18
2-ROH (W/OME,NaLS)	—	—	—	—	2.10
2-ROH (O/WME,CTAB)	—	—	—	—	1.85
2-ROH (W/OME,CTAB)	—	—	—	—	2.02

Table 8

Transient quenching constant (K_T) values (in $\text{mol}^{-1} \text{dm}^3$) and radii of the 'Quenching sphere of action' (in nm) of *O*-alkyl naphthyl ethers by BPM and BPH in oil-in-water microemulsions

Fluorophore	NaLS O/W ME				CTAB O/W ME	
	BPM		BPH		BPM	
	K_T ($\text{mol}^{-1} \text{dm}^3$)	R (nm)	K_T ($\text{mol}^{-1} \text{dm}^3$)	R (nm)	K_T ($\text{mol}^{-1} \text{dm}^3$)	R (nm)
1-ROCH ₃	86.0	3.24	51.0	2.72	173.31	4.09
1-ROC ₇ H ₁₉	84.6	3.22	44.4	2.60	155.50	3.94
1-ROC ₁₂ H ₂₅	80.4	3.17	45.0	2.61	157.63	3.96
1-ROC ₁₆ H ₃₃	86.2	3.24	42.6	2.57	156.89	3.96
1-ROC ₁₈ H ₃₇	85.3	3.23	38.6	2.48	159.72	3.98
2-ROCH ₃	39.5	2.50	39.3	2.50	nq	nq
2-ROC ₇ H ₁₉	30.7	2.30	29.5	2.26	nq	nq
2-ROC ₁₂ H ₂₅	30.2	2.29	29.3	2.26	nq	nq
2-ROC ₁₆ H ₃₃	29.4	2.27	31.2	2.31	nq	nq
2-ROC ₁₈ H ₃₇	29.8	2.28	26.2	2.18	nq	nq

effect of spacer on the quenching phenomenon can not be felt when the two picolinium moieties are separated by more than three methylene groups. This may be attributed to the extent of separation of charge in the quencher. The R values with Cu^{++} (concentrated charge only) are much less than that for the salt. The influence of salt can, therefore, be felt to a longer distance than with Cu^{++} .

3.6. 1-RO^{-*} in microemulsions

In view of the fact that microemulsions offer pockets for compartmentalization, 1-RO^{-*} remains in the water phase away from the interface in NaLS ME and close to the interface in CTAB ME. The quenchers, having positive charge and of varying hydrophobicity, may have various solubilization sites in the microemulsions. The order of decrease of K_T values of 1-RO^{-*} is found to be, CTAB (W/O) > CTAB (O/W) > water > NaLS (O/W) for BPM. It is reported that counterions with divalent charges separated by more than six methylene groups anchor at the micellar interface and decrease the CMC [16,17]. But when the charge separation is small, the counterions move radially over the charged micelle surface. Due to this the effective concentration of the quencher in bulk water is reduced resulting in a lower value of K_T for 1-RO^{-*} in O/W NaLS ME than for 1-RO^{-*} in water. Due to the negatively charged interface of NaLS, 1-RO^{-*} resides in the bulk water (Fig. 4) of the microemulsion, but in case of positively charged interface of CTAB, it resides near the interface (Fig. 4) of the microemulsion. Thus, for quenching of 1-RO^{-*} in CTAB microemulsion, the movement of the fluorophore is restricted and in NaLS microemulsion the movement of the quencher is restricted. The higher K_T values for 1-RO^{-*} in CTAB microemulsion is due to the free movement of the quencher (whose concentration is more than 100 times of that of fluorophore) in the microemulsion. The

higher value of K_T for W/O ME (CTAB) than O/W ME (CTAB) may be attributed to the concentration effect.

3.7. 1-ROH and 2-ROH in microemulsions

The solubilization sites of 1-ROH and 2-ROH are at the interface and in the mesophase respectively (Fig. 4) in the microemulsion droplet. The quenchers are in the bulk water and are away from the interface in CTAB ME whereas in NaLS ME these are close to the interface. The K_T (or R) values for 1-RO^{-*} is always higher than that for 1-ROH* in all the environments. This is because of greater distance of influence of 1-RO^{-*} than of 1-ROH*. The order of change of K_T values of 1-ROH in microemulsion is CTAB(W/O) > CTAB(O/W) > NaLS (W/O) > NaLS (O/W). The values are more in W/O ME because of concentration effect. 2-ROH is found to obey the SV equation in NaLS microemulsion throughout the experimental concentration. In this case, the quenching phenomenon may be due to the collision of the fluorophore with the quencher which is localized at the microemulsion interface. 2-ROH* is localized away from the interface and the quencher is associated with the interface of NaLS ME. In both the W/O and O/W NaLS microemulsions, the K_{SV} values are found to be independent of the medium and the spacer length of the quencher. As the quencher is localized in free water region and is away from the interface in CTAB microemulsion, there is no quenching. In NaLS microemulsion where the quenchers are bound to the interface, quenching occurs through collision. However, in CTAB microemulsions significant K_T values have been obtained when hexyl picolinium salt is taken as the quencher. In this case, the quencher anchors at the interface due to hydrophobic interaction of hexyl group of the quencher and hydrophobic tail of the surfactant. Behera et al. [18], while studying the interaction of CTAB with styryl pyridinium dyes having var-

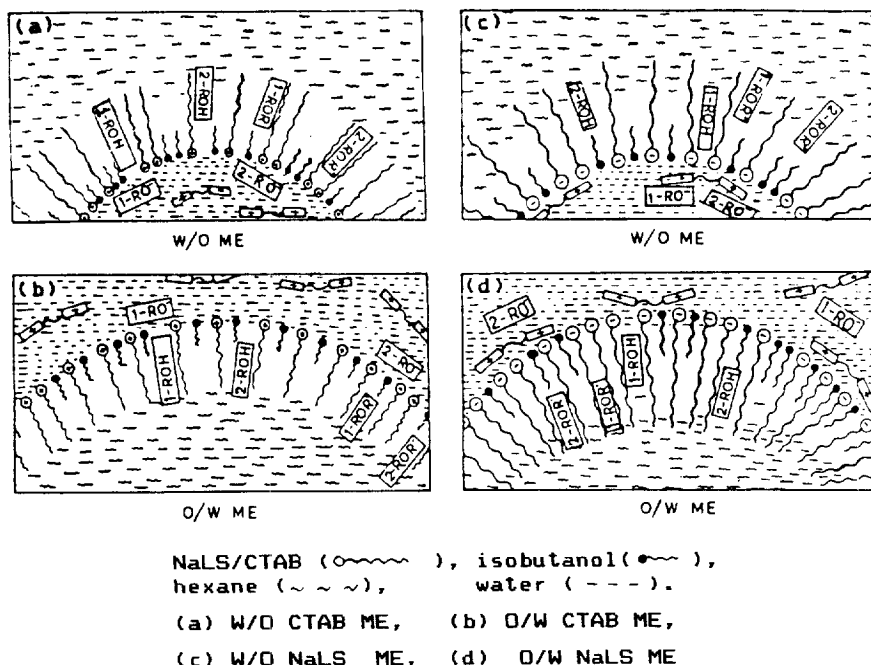


Fig. 4. Schematic representation for localization of fluorophores and quenchers in NaLS/CTAB–isobutanol–hexane–water system.

ied chain length have observed that when alkyl groups having six or more carbon atoms anchor at the interface due to insertion of the alkyl (hexyl) group into the mesophase. Hence quenching studies in CTAB and NaLS ME provide an unique example of distant effect.

3.8. *O*-alkyl derivatives of naphthols (ROR') in O/W ME

The transient quenching constant (K_T) and radii of the 'Quenching sphere of action' (R) values of *O*-alkyl naphthyl ethers with BPM and BPE salts in NaLS and CTAB O/W microemulsions are given in Table 8. The data in Table 8 brings out the following generalizations.

(a) The K_T values of 1-series decrease with increase in spacer length of the salt in NaLS microemulsion. Consequently the radius of the sphere of action also decreases.

(b) The K_T values of 1-series are higher than those of 2-series for both the BPM and BPE salts.

(c) The K_T values of 1-series in CTAB microemulsion is about two times higher than in NaLS microemulsion for BPM but are negligible with BPH as the quencher. The fluorescence of 2-series of compounds is not quenched by both the salts in CTAB microemulsion.

The fluorophores and the salts are compartmentalized in the microemulsion droplet. The 2-series of naphthyl compounds are more hydrophobic than 1-series and therefore are presumed to occupy a site deeper in the nonpolar domain than that for 1-series. The salts in NaLS ME are at the interface of the droplet owing to coulombic force of attraction. The 2-series of compounds have a lower K_T value than 1-series of compounds in NaLS (O/W) ME for both BPM and BPH

salts. Further the quenching in CTAB (O/W) ME with BPM salt has a higher K_T value than that for NaLS (O/W) ME. The BPH salt does not quench in CTAB ME. The results therefore can be explained taking into consideration the locational and orientational advantage of the fluorophore.

Acknowledgements

The authors thank the Department of Science and Technology, New Delhi (Grant No. SP/S1/F67/88) for funds and the Sambalpur University for providing facilities. One of the authors (MP) acknowledges the Council of Scientific and Industrial Research (CSIR) for providing a fellowship.

References

- [1] P.K. Dash, B.K. Mishra, G.B. Behera, Spectrochim. Acta A52 (1996) 349.
- [2] M. Panda, P.K. Behera, B.K. Mishra, G.B. Behera, Ind. J. Chem. 33A (1995) 11.
- [3] M. Panda, P.K. Behera, B.K. Mishra, G.B. Behera, J. Photochem. Photobiol. 90 (1995) 69.
- [4] Y. Moroi, Micelles Theoretical and Applied Aspects, Plenum, New York, 1992, p. 122.
- [5] M. Panda, P.K. Behera, B.K. Mishra, G.B. Behera, J. Lumin. 69 (1996) 95.
- [6] Vogel's Textbook of Quantitative Inorganic Analysis including Elementary Instrumental Analysis, in: J. Bassett, R.C. Denney, G.H. Jeffery, J. Mendham (Eds.), ELBS, Longman, London, 1978, p. 342.
- [7] S. Senapati, P.K. Dash, B.K. Mishra, G.B. Behera, Ind. J. Chem. 34A (1995) 278.
- [8] C.M. Harris, B.K. Selinger, J. Phys. Chem. 84 (1980) 1366.

- [9] D.W. Ellis, *J. Chem. Educ.* 43 (1966) 259.
- [10] H. Shizuka, S. Tobita, *J. Am. Chem. Soc.* 104 (1982) 6919.
- [11] J. Georges, *Spectrochim. Acta Rev.* 13 (1990) 27.
- [12] J.R. Lakowicz, *Principles of Fluorescence Spectroscopy*, Plenum, New York, 1986, p. 260.
- [13] J.M. Frank, S.J. Vavilov, *Z. Phys.* 69 (1931) 100.
- [14] N.J. Turro, *Modern Molecular Photochemistry*, Benjamin/Cummings, San Francisco, CA, 1978.
- [15] M. Kaneko, X.H. Hou, A. Yamada, *J. Chem. Soc., Faraday Trans. 1* 82 (1986) 1637.
- [16] Y. Moroi, R. Sugil, C. Akine, R. Matuura, *J. Colloid Interface Sci.* 108 (1985) 180.
- [17] Y. Moroi, N. Ikeda, R. Matuura, *J. Colloid Interface Sci.* 101 (1984) 285.
- [18] A. Mishra, S. Patel, B.K. Mishra, G.B. Behera, *J. Colloid Interface Sci.*, communicated.